Section 2
ADVANCED TECHNOLOGY DEVELOPMENTS

2.A A High-Repetition-Rate, Cr:Nd:GSGG Active-Mirror Amplifier

The active-mirror geometry amplifier was invented at General Electric[1] and developed at LLE in a program[2] that culminated in the deployment of a Nd:glass-active-mirror final-amplifier stage on the single-beam glass development laser (GDL) system.[3] These four 21-cm clear-aperture units produced 660 J in an 0.8-ns pulse[3] in single-shot operation. In the past year, a program has begun to develop the active-mirror geometry amplifier as a high-repetition-rate device.[4] This article describes the first results of that program.

A high-repetition-rate active mirror is shown schematically in Fig. 32.3. The mirror consists of a circular plate of the gain medium, cooled and pumped from one side by a length-tailored array of flash lamps. Key to the operation of the active mirror are the dielectric thin-film coatings applied to the plate. The coating on the rear (pumped) side of the plate is highly reflecting at the gain wavelength and highly transmitting at the pump wavelength. The front coating is the converse of the rear – highly antireflecting at the gain wavelength and highly reflecting at the pump wavelength. In operation, both the beam to be amplified and the pump light double pass the gain medium for efficient extraction and absorption. Cooling is done through a major face only, to ensure that with uniform pumping thermal gradients are parallel to the direction of propagation of the amplified beam. It is possible to simultaneously cool both major faces if a suitably transmissive coolant for the front can be identified. The circumference of the plate is angled and fine ground to defeat parasitic oscillation and reduce amplified

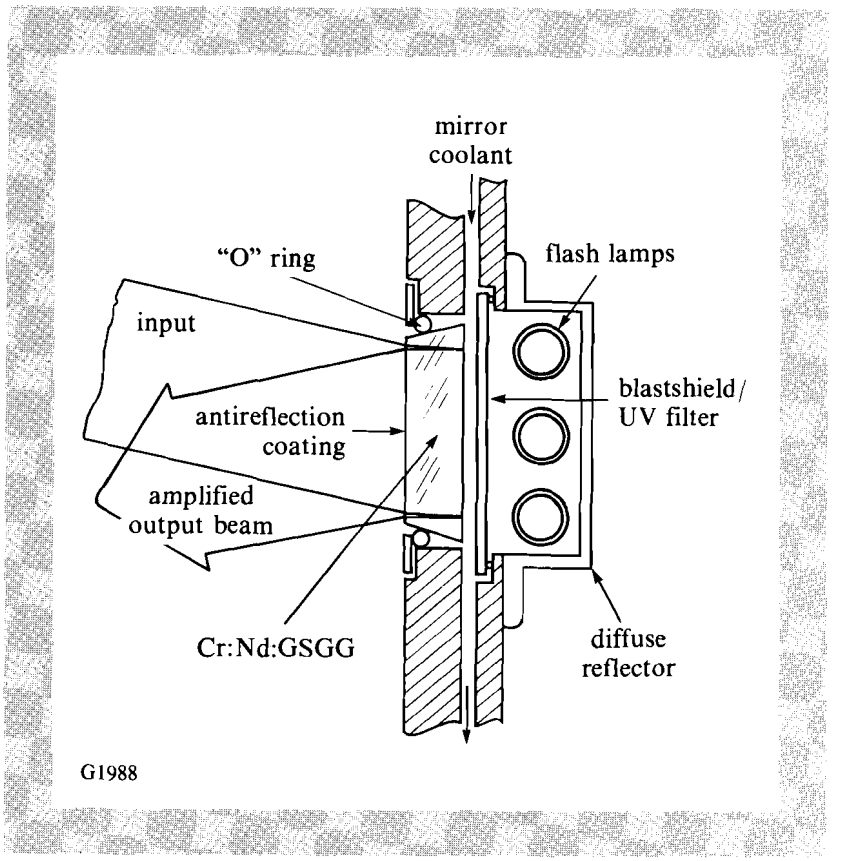

Fig. 32.3
High-repetition-rate active-mirror technology.

spontaneous emission (ASE) losses. The front and rear of the mirror are at a slight angle to deflect residual front-face reflections out of the amplified beam and to further discriminate against parasitics. A combination blast shield and UV filter protects the active medium from ultraviolet light emitted by the flash-lamp array.

The active-mirror geometry amplifier is a very attractive high-repetition-rate device from a number of standpoints. As already mentioned, propagation is parallel to thermal gradients, thereby eliminating dn/dT focusing when uniformly pumped. The active mirror is inherently double passed for both the laser and pump light. Compared to Brewster angle slabs, fabrication of the round plate is simple, which leads to lower costs. The clear aperture is round, eliminating the need for anamorphic transport optics. Finally, for a given clear aperture, the active-mirror geometry offers the shortest possible major dimension, thereby minimizing ASE difficulties. In order to enjoy these advantages of the active-mirror geometry, the moderate-gain path length and the thermal bending of the plate must be understood.

The co-doped crystalline material Cr^{+3}:Nd^{+3}:GSGG was chosen as the active medium. It offers a much higher effective stimulated emission cross section,[5] $\sigma(^4F_{3/2}-^4I_{11/2}) = 1.3 \times 10^{-19}$ cm^2, compared to that of the LHG-8 glass[6] used in the large active mirrors,[7] $\sigma = 4.0 \times 10^{-20}$ cm^2. This implies a higher small-signal gain per unit inversion. Co-doped GSGG was available in large core-

free boules with diameters of 4 cm at the time of acquisition (April 1986). It is thermally and optically isotropic when unstressed. The co-doping and effective energy transfer[8] from the Cr^{+3} to the Nd^{+3} increases pump absorption and reduces the very high pump powers needed with purely Nd^{+3}-doped crystals. GSGG has a high thermal conductivity characteristic of crystals, a large Young's modulus, and high fracture stress limit, which are summarized by the thermal stress resistance parameter R_S.[9] The R_S of GSGG[5] of 6.6 W/cm is half that of Nd:YAG but still over six times that of the LHG-5 glass.[6] Finally, for the active-mirror application, this material is readily coated with dielectric thin films.

The GSGG active mirror is 4.0 cm in diameter, with a 3.8-cm clear aperture defined by the coatings. The thickness was chosen to be 0.95 cm for purely mechanical reasons. This thickness allows mounting by a circumferential O-ring without deformation of the plate. The plate itself was cut from the boule, perpendicular to the boule's axis. The Cr^{+3} and Nd^{+3} dopings were 1 and 2 $\times$ 10^{20} ions/cc, respectively. These are vendor-supplied numbers.[10] The absorption through the plate at the peak of the Cr^{+3} 460-nm absorption band is in excess of OD 4. Although determining the optimum doping levels is a complex problem, requiring the balancing of absorption, plate thickness, Cr^{+3} to Nd^{+3} energy transfer, and concentration quenching, it is clear that these dopings, dictated by material availability, were high for the chosen plate thickness.

The GSGG plate was measured interferometrically prior to coating for transmitted wave-front quality. The transmitted wave front at 1 μm was less than 1/3 wave, peak to valley. This 1/3 wave was subsequently determined, by surface interferometry, to be almost entirely due to the edge rolloff characteristic of the polished material. There was also some high-frequency ($\sim$ 1-mm), very low contrast structure on the transmission interferograms. The source of this structure has not been determined.

The spatially resolved birefringence of the plate was measured at 632.8 nm, using a scanning-modulated transmission ellipsometer.[11] The plate was scanned across a diameter, using a 2-mm beam. The birefringence typically started at 0.7 nm/cm in the center of the plate, increased slightly to $\sim$1 nm/cm at a radius of 1 cm, and then decreased through zero to a value of $\sim$ -2 nm/cm at the edge of the plate. The circumference of the plate is initially in compression.

The fluorescence lifetime (1/e) of the Nd^{+3} was measured to be 280 ± 17 μs, using a standard apparatus in use at LLE for measuring Nd in glass lifetimes.

The plate is pumped by a shape-tailored array of three, 8-mm bore, 300-Torr xenon flash lamps. The top and bottom lamps (see Fig. 32.3) have a 1.5-in. arc length, and the middle lamp has a 2.0-in. arc length. The lamps are driven with a 300-μs, 1/3-current maximum-full-width, critically damped pulse. The maximum single-pulse energy is 460 J. A switch mode charger[12] provided 4 kW of power for the lamps. At

maximum bank energy, the peak repetition rate was 8.7 Hz; operation at 10 Hz was obtained by reducing the bank energy to 400 J. The lamps are mounted in a common flooded cavity.

The active-mirror head itself is modular in design. A single plate and compression ring hold the mounting O-ring for the GSGG. A 0.125-in. spacer plate defines the cooling channel. The active mirror is cooled with a 50/50 mixture of ethylene glycol and water. Typical flow rates are ~4 gal per minute. The flash-lamp array, UV filter, and blast shield assembly bolt over the coolant plate. The UV filter is a Schott[13] WG-320, 320-nm UV cutoff filter. The cutoff wavelength was chosen to be between the ~300-nm GSGG UV edge and the 346-nm Nd^{+3} absorption band.

The small signal gain was measured at the center of the active mirror as a function of bank energy. The probe beam was from a Q-switched GSGG oscillator with a pulse width of 0.5 μs, and was attenuated to ensure that the small signal gain was being measured. The measured gain did not change within the error bars when the input intensity was changed by a factor of 10 (i.e., an ND = 1.0 inserted into the beam). The gain was measured using the ratio of ratios technique,[14] which eliminates any errors due to probe fluctuations. Figure 32.4 shows the gain as a function of bank energy. The maximum gain measured was 1.61 ± 0.04. Overlaid with the data is a simulation of the expected small signal gain from the code TRENDE.[15] This code takes into account the time and wavelength dependence of the flash-lamp emission and the active material absorption spectrum. The simulation shown in Fig. 32.4 did not

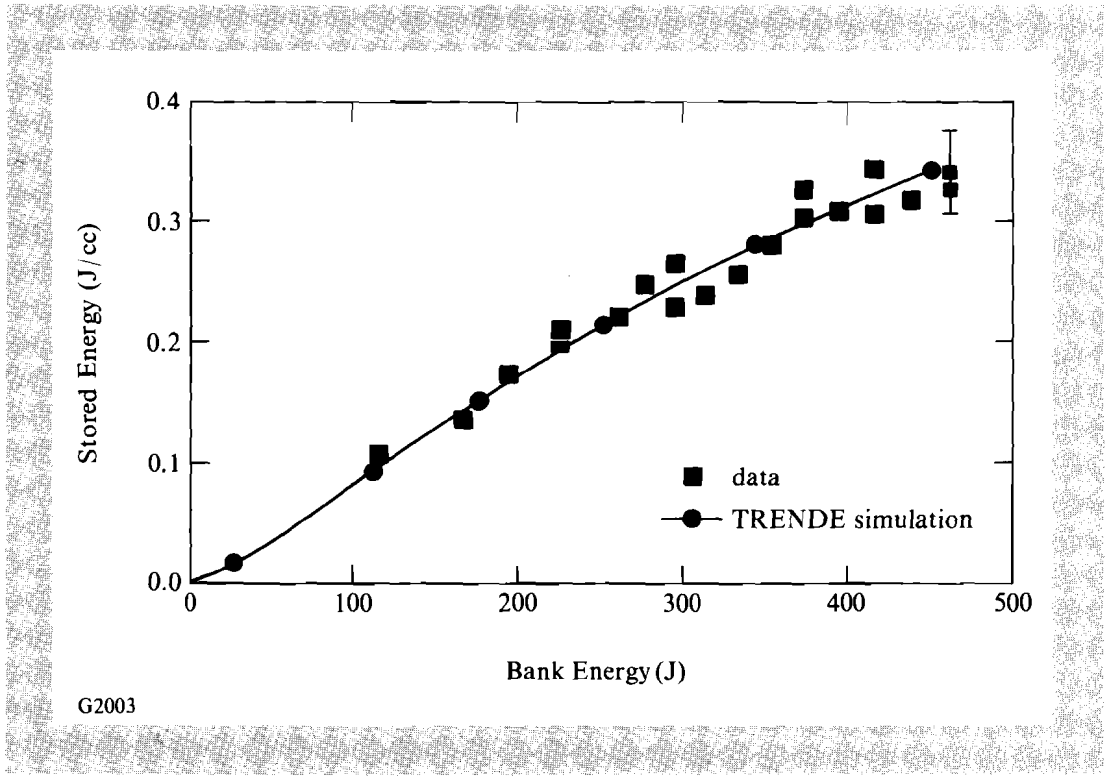

Fig. 32.4
Small signal gain versus bank energy, in joules.

invoke any ASE losses. Good agreement of the code with the experiment indicates that the device is not limited by ASE. The slight curvature that is seen in both the simulation and the data comes from the fact that as the flash lamps are driven harder, the pump spectrum shifts slightly to shorter wavelengths. TRENDE also calculates the inversion as a function of mirror thickness. By multiplying by the χ factor,[16] the inversion may be converted to heat deposition as a function of thickness.

Knowledge of both the stimulated emission cross section and the small signal gain allows calculation of the stored energy density in the mirror. Using a cross section of 1.3×10^{-19} cm^2, and a gain of 1.61, yields an average stored energy of 0.361 J/cm^3. If we multiply this value by the volume of the active mirror, we obtain the total energy stored in the upper lasing level that is accessible, assuming uniform pumping. This value has been calculated to be 3.9 J. If we assume an 80% fill factor and that we extract 75% of the energy, the total energy that can be added to a laser beam is found to be 2.3 J for this mirror. At a repetition rate of 8.7 Hz, this represents an average extractable power of 20 W.

The gain uniformity was measured by imaging the fluorescence of the mirror onto a CID camera.[17] The camera was placed approximately 40 cm away from the mirror to ensure that no vignetting of the image in the camera's lens system occurred, and it was double filtered with a three-cavity interference filter and an RG 1000 long-pass filter to guarantee that no pump light would reach it. The fluorescence was found to be parabolic in profile with the edge at 80% of the level at the center of the mirror.

Lateral-shearing interferometry[18] was performed on both a beam reflected from the front surface of the mirror and a beam passing the mirror material and reflecting from the rear surface. The front surface was sheared with a frequency-doubled YAG, which was reflected by the front surface coating. The total wave front was sheared with the same YAG without doubling. The slight wavelength difference between Nd:YAG at 1.064 μm and Nd:GSGG at 1.061 μm eliminated gain effects. Data was taken as a function of average pump power and recorded with a CID camera connected to a video cassette recorder. Lateral-shearing interferograms may be readily interpreted to yield the waves of defocus on the sheared beam in one dimension.[18] Interferograms were taken in both the horizontal and vertical directions and were found to be equal to within the error bars of the experiment (± 0.25 μm).

Thin-plate theory[19] predicts purely parabolic and equal (within a constant) surface displacements of a traction-free plate with a temperature variation through its thickness only. The thin-plate approximation is not valid in regions that are within one plate thickness of an edge. Because the thickness of the Cr:Nd:GSGG places a large fraction of the mirror near the edge, a finite-element code CYLLAS was written to predict the surface displacements. This code uses as input the thermomechanical properties of Cr:Nd:GSGG and the

TRENDE-computed energy deposition rate as a function of thickness. It solves the steady-state, Fourier heat conduction equation in one dimension, with the boundary condition that the front face is insulated and that the cooling of the rear surface may be approximated with a film coefficient. The computed temperature profile is then used to calculate the stresses, strains, and displacements. Once the displacements are known, a ray trace of the mirror is performed to determine the optical path difference (OPD) between center and edge.

Figure 32.5 shows the measured front surface displacement at the edge of the aperture due to defocus. Also shown on this figure is the CYLLAS-predicted displacement for a χ value of 2.0. Note the close agreement.

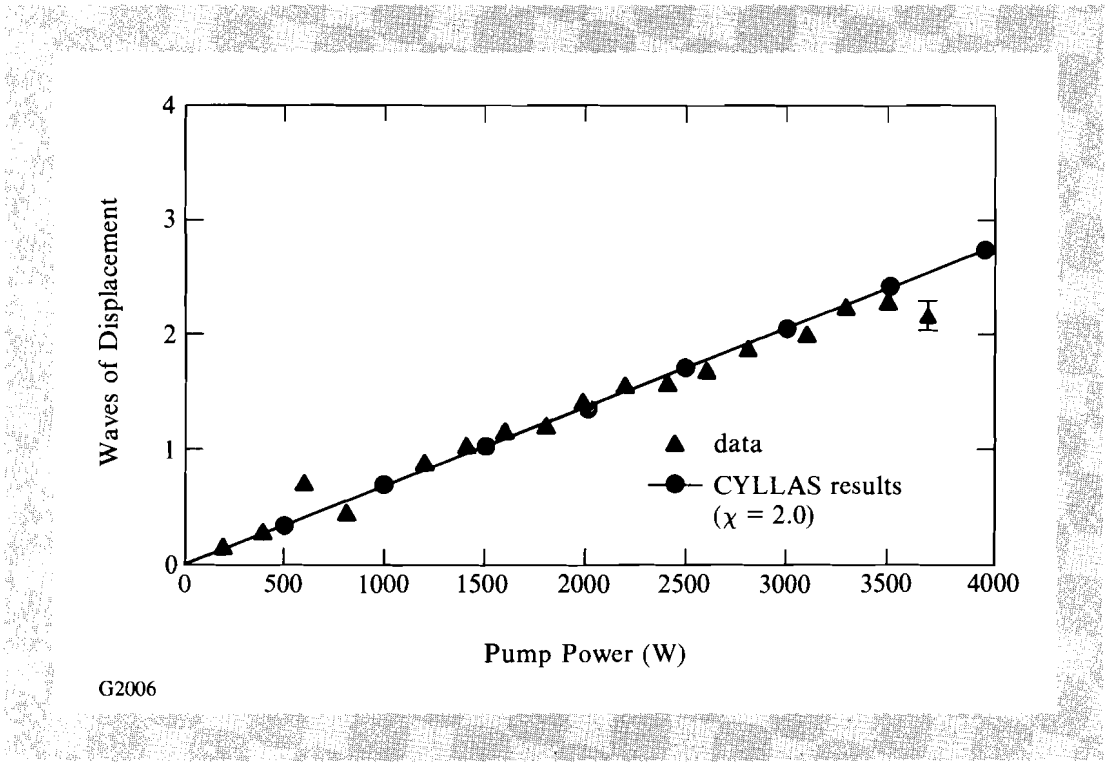

Fig. 32.5
Front surface edge displacement in waves at 1.06 μm versus average pump power in watts.

Figure 32.6 is a plot of the number of waves of defocus at the edge of the aperture on the beam reflected from the back surface versus pump power. Also plotted are the predictions of the code CYLLAS for two cases. In the first case, the mirror is assumed uniformly pumped and ~ 5 waves of defocus are predicted at maximum power. In the second case, a parabolic radial temperature profile with the edge of the mirror at 90% of the center temperature was assumed. In this second case, dn/dT^{20} was included in the OPD calculation and good agreement with the measured ~ 3 waves was obtained. While the steady-state bending of the mirror causes it to act as a negative lens, this is partially compensated for by the GSGG itself acting as a positive lens. The difference between the 20% center-to-edge decline in fluorescence and the inferred 10% center-to-edge decline in temperature is hypothesized to be due to radial direction heat conduction.

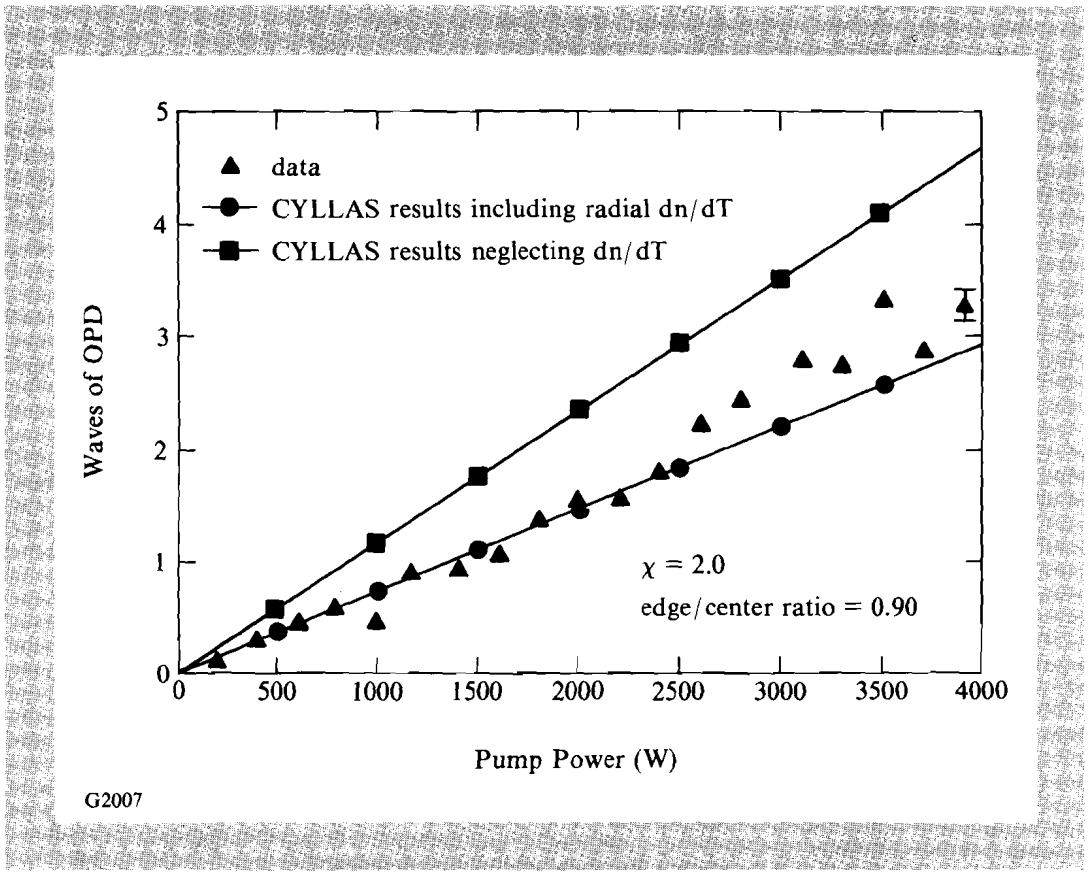

Fig. 32.6
Center-to-edge optical path difference in waves at 1.06 μm versus average pump power in watts.

As the mirror's pump power is increased, CYLLAS predicts that the circumference ($\sigma_{\theta\theta}$) will go into tension after overcoming the initial compression. The consequent stress-induced birefringence was probed by placing the mirror between crossed polarizers and measuring the transmission with a small beam, with the input polarizer at 45° to a radius. At the edge of the clear aperture, the transmission was 2.4% when unpumped, went down below 0.5% at 2-kW pump power, and then increased to 2.5% at full (4-kW) pump power. The 2.5% depolarization at the edge was the maximum observed in the clear aperture.

In conclusion, we have demonstrated the highest-repetition-rate (10-Hz) and highest-gain (1.6) active mirror published to date. This device is also the largest clear-aperture (3.8-cm) Cr:Nd:GSGG amplifier yet reported. Measurements of gain and wave front show good agreement with the theoretical models. New designs are being pursued for a next-generation, high-repetition-rate active mirror that will improve small signal gain, repetition rate, and wave-front quality.

ACKNOWLEDGMENT

This work is supported by Daewoo Heavy Industries of Incheon, Korea. The authors gratefully acknowledge the technical assistance of M. Tedrow and J. Suhan through all phases of the experiment.

REFERENCES

1. J. P. Chernoch, U. S. Patent No. 3 466 569 (9 September 1969).
2. J. A. Abate, L. Lund, D. Brown, S. Jacobs, S. Refermat, J. Kelly, M. Gavin, J. Waldbillig, and O. Lewis, *Appl. Opt.* **20**, 351 (1981).
3. T. Kessler, W. Seka, J. Kelly, D. Smith, R. Bahr, W. Lockman, N. Wong, and J. Soures, *High-Power and Solid-State Lasers* (SPIE, Bellingham, WA, 1986), Vol. 622, p. 156.
4. D. C. Brown, R. Bowman, J. Kuper, K. K. Lee, and J. Menders, *Appl. Opt.* **25**, 612 (1986).
5. W. F. Krupke *et al.*, *J. Opt. Soc. Amer. B* **3**, 102 (1986).
6. Product of Hoya Optics, Inc., 3400 Edison Way, Fremont, CA 94538.
7. S. E. Stokowski, R. A. Saroyan, and M. J. Weber, "Nd-Doped Laser Glass Spectroscopic and Physical Properties," prepared at Lawrence Livermore Laboratory under contract W-7405-Eng-48, 1978.
8. D. Pruss, G. Huber, and A. Beimowski, *App. Phys. B* **28**, 355 (1982).
9. J. M. Eggleston *et al.*, *IEEE J. Quantum Electron.* **QE-20**, 289 (1984).
10. Airtron, 200 E. Hanover Ave., Morris Plains, NJ 07950.
11. S. D. Jacobs, J. E. Hayden, and A. L. Hrycin, *Optical Thin Films II: New Developments* (SPIE, Bellingham, WA, 1986), Vol. 678, p. 66.
12. A. L. E. Systems model 302L, A. L. E. Systems Inc., 150 Homer Avenue, Ashland, MA 01721.
13. Schott Glass Technologies Inc., 400 York Avenue, Duryea, PA 18642.
14. J. V. Meier, N. P. Barnes, D. K. Remelius, and M. R. Kokta, *IEEE J. Quantum Electron.* **QE-22**, 2058 (1986).
15. J. H. Kelly, Ph. D. thesis, University of Rochester, 1980, available from University Microfilms International, Ann Arbor, MI 48106.
16. M. S. Mangir and D. A. Rockwell, *IEEE J. Quantum Electron.* **QE-22**, 574 (1986).
17. General Electric model 2505-A3, G. E. Co., 890 7th St. North, Liverpool, NY 13088.
18. D. Malacara, *Optical Shop Testing* (Wiley, New York, 1978), p. 105.
19. B. A. Boley and J. H. Weiner, *Theory of Thermal Stresses* (Wiley, New York, 1960).
20. J. C. Lee and S. D. Jacobs, *Appl. Opt.* **26**, 777 (1987).